Radio Science, Volume 36, Number 2, Pages 247–259, March–April 2001

Assimilation Ionosphere Model: Development and testing with Combined Ionospheric Campaign Caribbean measurements

J. J. Sojka, D. C. Thompson, and R. W. Schunk
Space Environment Corporation, Logan, Utah

T. W. Bullett
Battlespace Environment Division, Air Force Research Laboratory, Hanscom Air Force Base, Maryland

J. J. Makela
Department of Electrical and Computer Engineering, Cornell University, Ithaca, New York

Abstract. Assimilation Ionosphere Model (AIM) is a physics-based, global, ionospheric specification model that is currently under development. It assimilates a diverse set of real-time (or near-real-time) measurements, such as ionograms, GPS slant total electron content (TEC), and in situ plasma measurements. This study focuses on a middle latitude ionosonde assimilation capability in both local and regional forms. The models described are capable of using the f_oF_2 and h_mF_2 from ionograms to generate either a local or a regional distribution of the induced plasma drift. This induced drift is usually caused by the meridional neutral wind. Results from a local model (AIM1.03L) and a regional model (AIM1.03R) are presented and compared with the international reference ionosphere (IRI) climatological predictions as well as GPS slant TEC measurements. Results from year-long studies during solar maximum show that the accuracy of the AIM1.03L model is about a factor of 2 better than that of IRI. An initial month-long regional study is also presented, and the results are almost as good. A study is also carried out using observations taken during the Combined Ionospheric Campaign (CIC) held in November, 1997, in the Caribbean. The digisonde located at Ramey Solar Observatory is used to drive the AIM1.03L model, and the predicted GPS slant TECs are compared to those observed by a GPS receiver located at St. Croix. This study confirms that this first step in preparing a weather-sensitive ionospheric representation is superior to a climatological representation. This sets the stage for the development of full assimilation of GPS TEC, in situ density measurements, etc., and it is anticipated that the AIM1.03L-R ionospheric representation will provide an accurate ionospheric specification.

1. Introduction

The need to consider assimilation techniques for the ionosphere arises because present-day ionospheric specification techniques have been unable to attain the desired accuracy. On the one hand, empirical models, such as the international reference ionosphere (IRI) [*Bilitza et al.*, 1979; *Bilitza*, 1990] model, represent the monthly median climatology very well. Physical models, such as the Utah State University Time Dependent Ionospheric Model (TDIM) [*Schunk*, 1988; *Sojka*, 1989], were specifically designed to handle ionospheric weather but, because of a lack of weather input information, are also unable to accurately specify the ionospheric weather. Assimilation techniques rely on the availability of ionospheric observations of the parameters being modeled in near real time and on an initial specification of the ionosphere. When this information is combined by a numerical iterative scheme, such as a Kalman filter, it will provide an optimized ionospheric specification [*Daley*, 1990].

For Kalman filter assimilation procedure an extensive set of observations and a reasonably good initial estimation of the ionospheric specification are needed. It is only recently, via Internet-type communications, that multiple sources of real-time data can

Paper number 1999RS002411.
0048-6604/01/1999RS002411$11.00

be considered as practical real-time input for a model. Similarly, the approximate tuning of the initial estimation using a physical model running in real time is now possible because of increased speeds on work stations–PCs. The Assimilation Ionosphere Model (AIM) is a first step in producing a fully operational ionosphere model based upon the assimilation technique [*Schunk et al.*, 1997]. In this paper, only a small aspect of this task is described. The development only tackles the midlatitude F layer dynamics, in which, to a very good approximation, the F layer is primarily responding to neutral winds and only occasionally to $E \times B$ drifts. From a research perspective this ionospheric response was outlined in detail by *Rishbeth* [1967], and a practical procedure for deriving the plasma drift driver using ionosonde data was described by *Rishbeth et al.* [1978]. This technique is referred to as the servo technique [*Rishbeth et al.*, 1978]. The servo technique was applied by *Miller et al.* [1986] to determine the neutral winds at midlatitudes from measurements of the F layer peak height, h_mF_2. This demonstrates an aspect of our assimilation philosophy, that in order to successfully produce a final ionospheric specification, it is necessary to have a very good initial estimate that needs to be better than an empirical climatological state. Since the real-time observation capability will always leave room for improvement in both quality and coverage, it places an even greater significance on the quality of the initial ionospheric specification. The dynamics of the midlatitude ionosphere is dominated by an induced plasma drift, either from neutral winds, $E \times B$ drifts, or topside fluxes. If real-time data can be used to determine this drift input on a local, regional, or global scale, the ensuing physical ionospheric model will generate a very good initial ionospheric specification.

In this initial study, AIM simulations that are based upon ionosonde observations are presented. These are compared both with other observations and with other ionospheric models. The other observations include additional parameters obtained from the ionosonde data as well as the original data used to assimilate the plasma drift model. This has the problem of being considered incestuous. However, because of data quality issues, as well as model limitations, this comparison does not produce complete agreement and hence is a relevant topic of study.

Section 2 outlines how the AIM1.03L and AIM1.03R models differ from the classic servo technique outlined by *Rishbeth et al.* [1978]. In section 3, year-long ionosonde data sets are used to drive a local assimilation, AIM1.03L, while in section 4, ionosonde data over a 1000 km range are used to drive a regional assimilation, AIM1.03R. The CIC Caribbean study period of November 1997 is used for an AIM1.03L study during a geomagnetic storm. This study is presented in section 5 and includes a comparison with independent GPS TEC data. The results of this initial step in ionospheric assimilation are summarized in section 6.

2. Midlatitude Drift Assimilation

The standard servo model determines the induced plasma drift via its effect on the height of the F layer peak. *Miller et al.* [1986] in their Figure 1 show how the layer height changes from 250 km to over 400 km as the horizontal meridional neutral wind at Arecibo ranges from -100 to 100 m/s. Hence, by measuring h_mF_2, the F layer peak height, and referencing it to a zero-wind height, information about the induced plasma drift can be obtained. Various studies have been carried out to determine how best to relate this height difference to a drift [*Buonsanto*, 1990; *Richards*, 1991; *Titheridge*, 1995]. The difficulty in obtaining accurate results from the servo technique has also been discussed by these authors. Servo scaling parameters vary with local time as the physical processes at work in the bottomside ionosphere change. At both dawn and dusk the rapid altitude changes in photoionization due to terminator effects can lead erroneously to implied plasma drifts when a servo technique is used. Daytime and nighttime conditions also produce different F layer responses to these plasma drifts. *Buonsanto et al.* [1997] carried out an extensive comparison of the different applications of the servo technique, as used to derive the neutral meridional winds from ionospheric data. These different techniques were, in fact, variations on the original servo idea and involved a sequential set of estimates of meridional neutral wind in local time. These calculations could, in some cases, compensate for terminator effects.

Unfortunately, the ionosphere has relatively complicated altitude dependencies, which manifest themselves in one form as a height dependence of production, recombination, and diffusion rates. These processes can effectively be thought of as drivers of the plasma time constant. The time constant varies from less than a second in the E region to many minutes above the F_2 peak. If the neutral wind driver

is time varying on timescales less than 30 min, it is unlikely that the F layer can be assumed to be a sequence of diffusive equilibrium states; that is, the layer is still dynamically adjusting. Hence, at a subsequent time step the derivation of an induced plasma drift and meridional wind would depend on how the last step dynamics is still adjusting the F layer. This implies that a servo model with a constant coefficient will be unable to track all ionospheric weather conditions. If high accuracy is needed, then the coefficient must be adjustable on the basis of ionospheric history. Qualitatively, this can be understood by considering two scenarios in which the prior servo step had required, in one case, a meridional drift increased by 50 m/s and, in the other case, a meridional drift decreased by 50 m/s. In both cases, the ionosphere dynamically responds and redistributes plasma in opposite ways. These cases might well yield different effective coefficients in the servo. If, on the other hand, both drifts had only a magnitude of 5 m/s, a single coefficient would suffice. In principle, such considerations can be implemented in a servo. However, how these effects would then be propagated forward in time to the next servo step becomes complicated, almost to the point of being nonlinear. This dependence on rapid change in the ionosphere is discussed by *Richards* [1991], where improvements to the basic servo scheme are described.

The key parameter in the servo simulation is h_mF_2. Unfortunately, in analyzing ionograms this parameter is the last profile parameter to be determined. The retardation of the radio wave at h_mF_2 is the integrated effect of all the plasma between this height and the ground. It requires that a full ionogram be available, and probably one that is free of noise in the form of spread conditions or signal dropouts. In real-time applications, even the most sophisticated software packages have difficulty reliably extracting this parameter all the time. For these reasons, associated with data quality, it is difficult to develop a real-time ionospheric ingest algorithm based only on h_mF_2 derived automatically from an ionosonde, especially when the quality of h_mF_2 is both variable and unknown.

The AIM philosophy is to maximize the usage of quality-controlled data and the use of ionosphere expertise to maximize the ingestion of these data in producing a best initial representation of the ionosphere. Within an ionosonde data set, in addition to h_mF_2 there is an f_oF_2 parameter as well as an entire bottomside profile. *Miller et al.* [1986] showed that h_mF_2 depends upon the vertical drift. In addition, they showed that f_oF_2, the peak density represented as a plasma frequency, is also dependent on the drift. In fact, the entire bottomside shape and height depend upon the induced plasma drift. AIM, in ingesting the ionosonde data, makes use of these correlations such that in the absence of a clear peak signature in the ionogram the bottomside can still be used to drive the assimilation. In most cases, f_oF_2 is known to have a better accuracy than h_mF_2. At certain times of the day, h_mF_2 becomes uncertain because the density profile may be very broad and flat around the peak, which further compounds the problem of obtaining an accurate h_mF_2. Hence f_oF_2 is emphasized over h_mF_2 during ingestion.

The AIM midlatitude development began with a local station servo model using only h_mF_2. This model was referred to as AIM1.01L. As expected, it was found to be inadequate, so the h_mF_2 analysis is augmented with f_oF_2 data. This was also in a classical servo model, AIM1.02L, but this was only a slight improvement. The remaining problem is that when the conditions change rapidly, the past history dynamics still influence the next step [*Richards*, 1991].

At this point we discarded the conventional servo technique and developed an entirely different approach. The new approach was based on the need to avoid introducing rapid changes in the F region drivers. Hence a "one-pass" servo scheme cannot be used. Instead, an iterative scheme was adopted. Although the CPU demands are significantly more intensive, this scheme "creeps" toward a solution consistent with the F region ionosonde observations. The first assimilation of this new type used only f_oF_2 and h_mF_2 as inputs and is referred to as AIM1.03L. This model was used for all the local assimilations represented in sections 3–5. A by-product of each local assimilation is the vertical induced plasma drift. This, in turn, is merged with other ionosonde assimilated vertical drifts to produce a regional drift description, which is then used to drive a regional ionospheric specification (AIM1.03R).

3. Local AIM1.03L Studies

The first application of the AIM1.03L development was based on data obtained from 24 midlatitude ionosonde stations over 2 complete years. The ionosonde data f_oF_2 and $M3000$ were obtained from the National Geophysical Data Center ionosonde CD-ROM database. These data are hourly values. Both a

Table 1. Group 2 Ionosonde Stations

Station Name	Identifier	Geographic Latitude, deg	Geographic Longitude, deg
Wakkanai	WK545	45.4	141.7
Akita	AK539	39.7	140.1
Kokubunji	TO535	35.7	139.5
Yamagawa	YG431	31.2	130

solar maximum year, 1981, and a solar minimum year, 1985, were chosen for the study period. Ionosondes were selected on the basis of being a midlatitude station (magnetic latitudes from 28° to 55°), the availability of f_oF_2 and $M3000$ exceeding 90% for both years, and stations forming local groups that would enable regional assimilation schemes to be tested.

For the purposes of this paper only data from group 2 stations will be discussed and presented. Table 1 lists the key information for the four ionosondes from group 2. This group is used because the stations have an excellent spacing in latitude and almost none in longitude. Figure 1 shows the geographic locations of these four stations. For this study, it is primarily Kokubunji, Akita, and Wakkanai that are used, and these three are almost lined up on the same longitude. Excellent spacing in latitude refers to a distance of ~500 km (5° in latitude), which is about half the usually quoted coherence length of midlatitude ionosphere structure and variations. The first step of the AIM procedure was to control the ionosonde data stream for quality. A very rudimentary flag system was used to identify bad data and missing data. The second stage in this case was to convert the $M3000$ values to h_mF_2. This was accomplished using the algorithms presented by *Dudeney* [1974], specifically equation (56) in that publication.

Unfortunately, this algorithm needs the E region f_oE in addition to f_oF_2. The f_oE values are infrequently available, and as a default, a physical ionosphere model (Ionospheric Forecast Model) was used to generate the f_oE. The single-station assimilation process consisted of two phases: The first involved the comparison of modeled and observed f_oF_2 and h_mF_2 and then an adjustment of the model inputs. This process, as indicated in section 2, was then slowly iterated to obtain convergence. The assimilation process in this example was therefore very straightforward. It involved indices Kp and $F10.7$, two observational inputs that have a relative weighting that is adjustable (depending on data quality), and then one internal driver parameter, i.e., the neutral wind induced plasma drift along the field line. After assimilating the observations to produce the induced drift the physical model was rerun with the new time-varying induced drift to produce the full ionospheric altitude profile from 90 to 1000 km.

Naively, one would then expect that the model outputs would be in 100% agreement with the observations; however, this is not the case. Simple considerations are revealing in this context; the sunrise f_oF_2 enhancement occurs rapidly with up to a 5 MHz change in f_oF_2 in 1 hour. The CD-ROM ionosonde data are "hourly" values. To date, we have been unable to obtain a unique confirmation of what this hourly value represents. Is it an hourly average, the f_oF_2 at the middle of the UT hour, or the best value for that hour? In the real world, f_oF_2 increases exponentially before rolling over to daytime values. The physical model can reproduce this, but at this time the input data are probably being erroneously used to identify this rapid sunrise effect. In a more general sense, both f_oF_2 and h_mF_2 (computed from $M3000$) show very marked fluctuations from hour to hour. What is the source of this fluctuation? Is it errors in ionogram scaling? Is it always a measure of ionospheric weather? The strong variability present in observed f_oF_2 and h_mF_2 is such that the physical model is unable to track them either individually or together when constrained to using only the vertical induced plasma drift as a free parameter. Hence

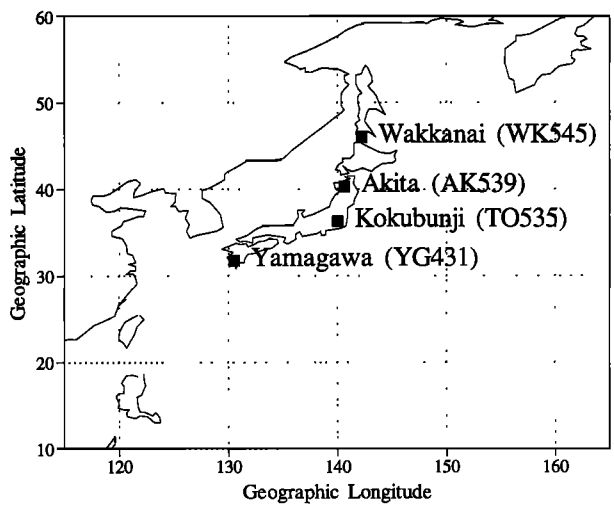

Figure 1. Map of the station locations from Table 1. Each station is in Japan and is labeled both by name and by international station code, in parentheses.

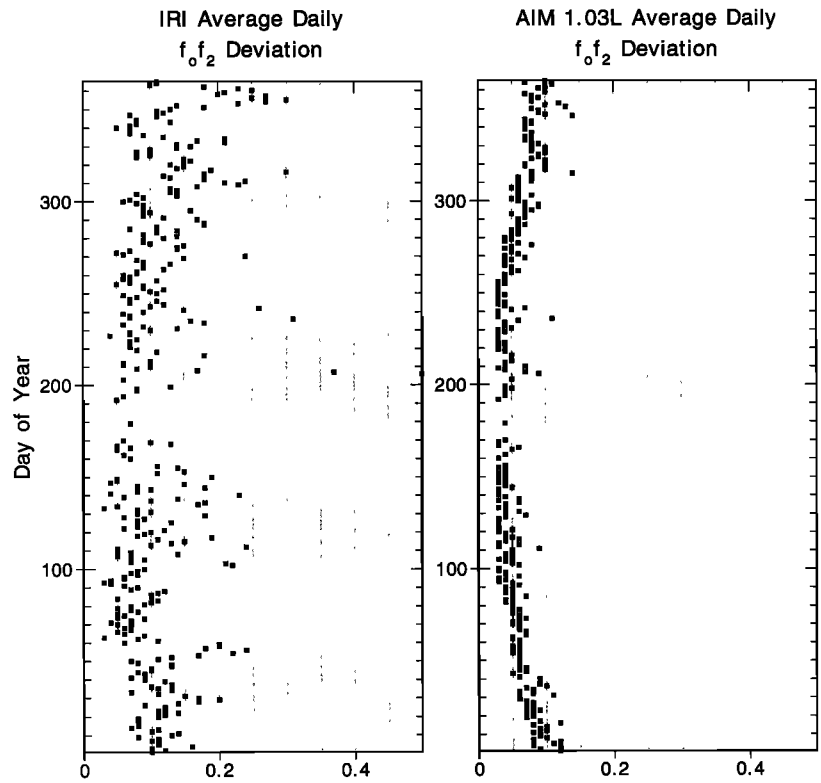

Figure 2. Daily f_oF_2 deviation between (left) IRI and Akita ionosonde f_oF_2 and (right) AIM1.03L and Akita ionosonde f_oF_2 for 1981. The daily deviation is expressed as an average of the hourly ratios of the deviation to the observation.

differences between input data and the AIM1.03L fit to the data exist. In one sense, the fluctuations represent a measure of the error in modeling the observations, i.e., the unmodeled effects.

With such caveats in mind, Figure 2 shows the 1981 observed f_oF_2 compared with IRI (left panel) and AIM1.03L (right panel). IRI is used here since it represents the international community's most accessible ionospheric model. It is based upon monthly median data and therefore can only represent climatology. Figure 2 is for the midlatitude station Akita, and 1981 was chosen because it was a geomagnetically disturbed year at solar maximum. Each point in Figure 2 represents the "daily average" of the hourly absolute deviation between the model and observed f_oF_2 relative to the observed f_oF_2. In Figure 2 the horizontal axis is labeled as a ratio, where 0.2 and 0.4 correspond to 20 and 40% daily average deviations, respectively. The IRI differences range from 5 to 25%, with a few disturbed days exceeding 25%. The spread in day-to-day values for IRI represents the effect of geomagnetic activity, which is not built into the "monthly median" IRI model. In contrast, the AIM1.03L obtains daily agreement in f_oF_2 to 3–5%. However, in winter the agreement is up to 10%. This, in fact, highlights a limitation of this particular physical model, which contains an insufficient nighttime maintenance of the F region, in this case, an absence of interhemispheric plasma flow. Even with this limitation, the AIM1.03L reproduces the F layer peak density to better than 10% in summer and better than 20% in winter. These uncertainties in density are propagated from the f_oF_2 uncertainties using the fact that the density is proportional to the square of the frequency. In contrast, the IRI density comparison ranges from no better than 10% to 50%. From Figure 2, right panel, it is also evident that AIM1.03L tracks both the quiet and storm days consistently insofar as one cannot distinguish between days. In the IRI comparisons the monthly medium values are unable to track storms, and hence large deviations occur on storm days. AIM1.03L, in addition to recovering the

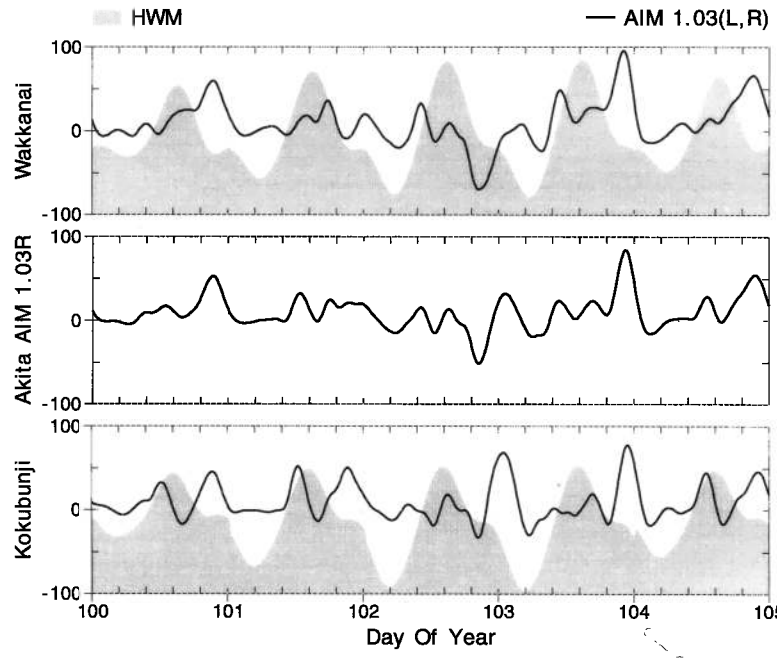

Figure 3. (top) AIM1.03L induced plasma drifts at Wakkanai, (middle) assimilated induced plasma drifts at Akita, and (bottom) AIM1.03L induced plasma drifts at Kokubunji. The corresponding induced drifts derived from the *Hedin et al.* [1991] wind model are shown as the upper boundary of the shaded region.

F layer parameters h_mF_2 and n_mF_2 (f_oF_2), also provides a full altitude distribution from 90 to 1000 km, its composition, its temperature, and the effective induced plasma drift. The AIM1.03L also fills in data gaps and, to an extent, because it includes realistic chemistry-plasma time constraints, does not follow rapid fluctuations that may well be measurement errors and unmodeled dynamics.

4. Regional AIM1.03R Studies

Single-station modeling, AIM1.03L, is not really assimilation. A more realistic scenario is to consider many stations (in our case, two) and then carry out an assimilation such that the induced drift between the stations can be determined from only these two points. Then, predict the f_oF_2 at the middle location, which can be compared with an observation from a third station at that middle location. The group 2 stations listed in Table 1 are ideal for this. Wakkanai and Kokubunji are used as the two endpoints. They are separated in latitude by 9.7°, which corresponds to 1150 km, and they are also both effectively at the same longitude. These two stations were used to generate locally the induced plasma drift. A 5 day example of this is shown in Figure 3. The shaded regions represent the physical model's default values for the induced drift when no data are available for assimilations. These default values are based upon the *Hedin et al.* [1991] wind model. The induced drifts from the two stations were then assimilated into a regional drift model that produced induced vertical drifts over an entire region, not just at the two end sites. The predicted drift is shown in the middle panel for the middle location, namely, the Akita station. Using this drift, the Akita ionosphere was then modeled. This entire regional assimilation capability is referred to as model AIM1.03R.

Plate 1 displays the diurnal f_oF_2 variation from day 100 to 109, in 1981, for the ionosphere over Akita. Plate 1a is the observed f_oF_2. This includes a data gap in day 101 from 0800 to 1200 LT. In this 10 day period the noontime (around 0600 UT) f_oF_2 varies from as low as 10 MHz to over 13 MHz. This is in response to storm activity on specific days. Plate 1d shows the climatology prediction from IRI, which, since it is based on monthly median data, is static over this 10 day period, although the diurnal variation appears adequate. The AIM1.03R simulation (Plate

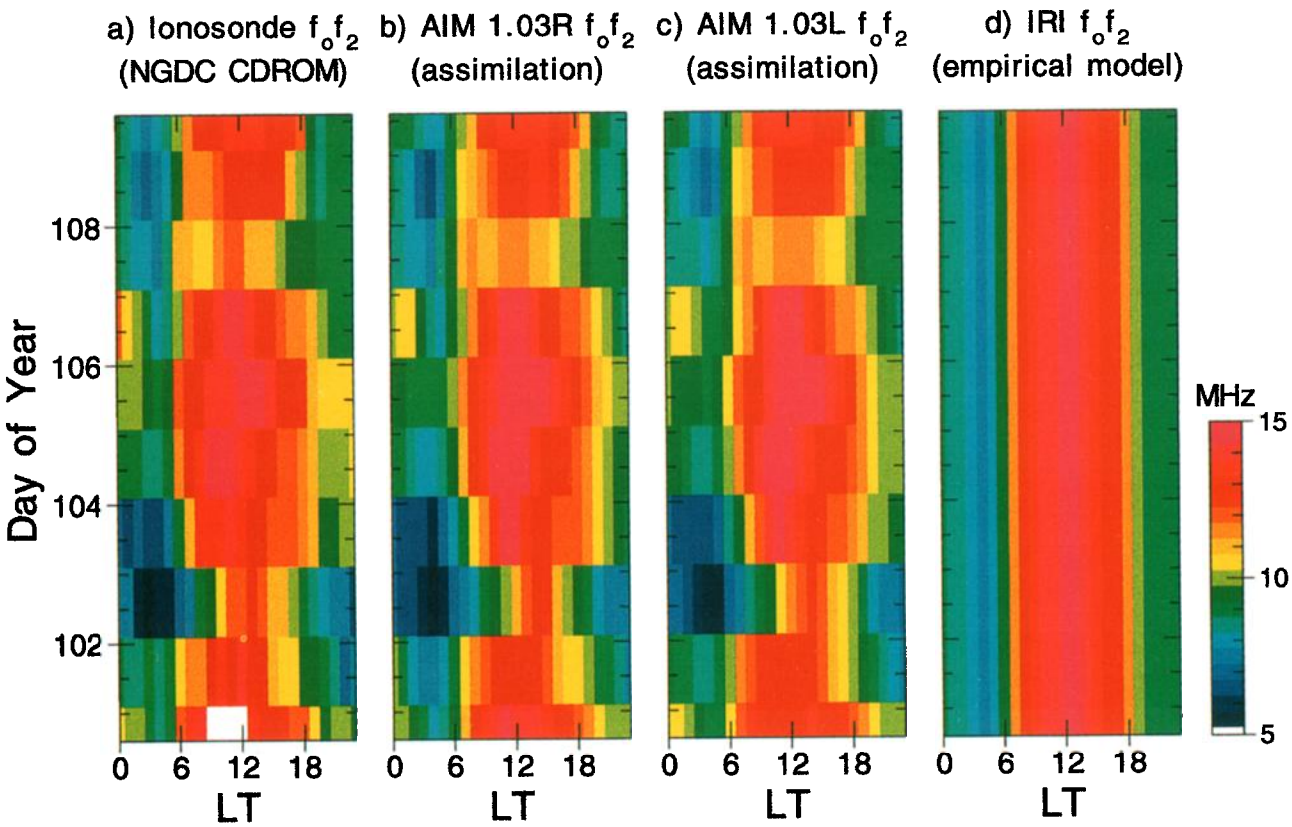

Plate 1. (a) Observed hourly Akita f_oF_2 for days 100–109, 1981, (b) regional AIM1.03R f_oF_2, (c) local AIM1.03L f_oF_2, and (d) IRI f_oF_2.

1b) contains no information from Akita, but information from two stations about 500 km away to the north and south. The driver that is based on these other two stations is shown in Figure 3. Hence the entire structure produced in Plate 1b is due to this "regional" assimilated induced drift.

For reference in this study, it is possible to use the Akita ionosonde data directly to drive a local assimilation, AIM1.03L. This, in fact, has been done and is shown in Plate 1c. The comparisons between the AIM1.03R, AIM1.03L, and ionosonde f_oF_2 are rather straightforward. Both assimilation models fill the gap in the data. Both models also reproduce the day-to-day variability rather well. In contrast, the IRI only demonstrates the diurnal climatological level. The study shown in Plate 1 was run for more than a one-month period with similar results. The "deviation" analysis shown in Figure 2, which was for a whole year, was also applied to this one month of AIM1.03R analysis. Table 2 summarizes these results in terms of a daily deviation when models are compared to observations, and an average is obtained for the entire year 1981.

In this tabulated form and from the day-to-day tracking it is evident that the AIM1.03R is able to reproduce the F layer peak from observations being made over 500 km away. Future testing will ascertain the actual coherence scales. These future studies will include both latitude and longitude distributions of stations to determine how best to assimilate the induced drift. In Figure 3 a rather straightforward approach was taken because all these stations lay on the same meridian.

Table 2. Daily Deviation at Akita Averaged Over 1981

Model	f_oF_2 Deviation, %	N_mF_2 Deviation, %
IRI	11	22
AIM1.03L	5	10
AIM1.03R[a]	6	12

[a]Averaged over only one month.

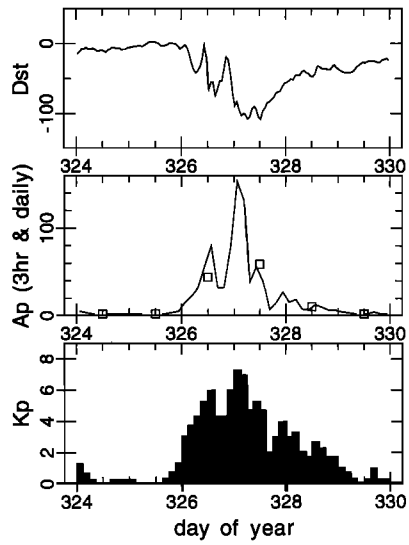

Figure 4. Geomagnetic indices (top) *Dst*, (middle) *Ap*, and (bottom) *Kp* for days 324 (November 20) to 329 (November 25), 1997.

5. November 1997 CIC Caribbean Campaign

A critical aspect of developing AIM or other potentially real-time assimilation models is that they must be robust enough to handle real-time data streams. Real-time data streams will not be quality controlled by experts. The operational environment and mode of observation or system performance of a real-time sensor can change abruptly and potentially not be corrected by an operator for hours or days. Yet the assimilation software must be able to handle these data quality conditions. In sections 3 and 4, quality-controlled ionosonde data streams were used. In this section, a more realistic operational assessment is made of how the AIM1.03L responds to a representative real-time ionosonde data stream under both quiet and disturbed geomagnetic conditions.

The November 1997 Combined Ionospheric Campaign (CIC) ran through the storm period of November 21–23. Figure 4 shows the *Dst*, *Ap*, and *Kp* geomagnetic indices from November 20 to 25 (days 324 through 329). The *Dst* index began its negative storm excursion at almost 0000 UT on November 22 and continued to go negative in a set of surges until ~1200 UT on November 23, when it reached a value of −100 gamma. The *Kp* variation indicates that the disturbed conditions remained almost above 4 for 2 days, while the *Ap* 3 hour index almost reached 160 at 0000 UT on November 23. In contrast, the first 2 days, November 20 and 21 (days 324 and 325), were classically quiet days. November 25 (day 329), which was in the recovery phase of the storm, almost reached the quiet level.

The instrument complement of the CIC Caribbean included an advanced digital ionosonde sounding system (DISS) located at Ramey Solar Observatory (18.5°N, 292.9°E) in Puerto Rico. This instrument generated the input data stream for the AIM1.03L simulations. Independently, the CIC Caribbean instrument complement also included several GPS-TEC receivers. Specifically, the one located at St. Croix (17.8°N, 295.4°E) was used as an ionospheric reference for this study period. The two GPS receivers used in the campaign are part of the Continuously Operating Reference Station (CORS) network. Our study began by ingesting the DISS data into AIM1.03L, creating a complete local profile of the ionosphere, computing slant TECs for each GPS satellite observed by the St. Croix receiver, and then comparing the AIM1.03L slant TEC with the St. Croix observations. In addition, comparisons were made to the IRI inferred slant TEC. A major assumption made in this initial study was that the instantaneous AIM1.03L Ramey vertical electron density profile was representative of the entire region through which the St. Croix GPS receiver slant paths cut. The study by *Makela et al.* [this issue] showed this assumption to be incorrect, especially during the storm main phase. However, handling the spatial ionospheric structure was beyond the current AIM1.03L development.

Figure 5 shows the Ramey Air Force Base (AFB) DISS f_oF_2 data during the study period. These data were the outputs of the Automated ARTIST ionosonde inversion program, which runs in real time on the DISS sounder. They have not been "cleaned up" by an ionosonde expert, so they do represent the level of raw data that operational software would have to work with. The first 2 days, days 324 and 325, show a well-defined nighttime ionosphere followed by day f_oF_2 variations. However, beginning at ~1000 UT on day 326, the storm effect becomes evident. On days 326, 327, and 328 the daytime f_oF_2 are all enhanced by over 3 MHz from the initial quiet days. During nighttime the f_oF_2 values are even more surprisingly enhanced and structured. A prenoon enhancement is present with almost quiet day postnoon (~1900 UT) values, and then a late afternoon evening enhancement occurs, leading to very enhanced nighttime

values. For almost 3 days during the storm and its early recovery, Ramey DISS observed an extended positive ionospheric storm phase. The Ramey DISS data do not display a negative storm phase during this storm.

Plate 2 shows the results of running AIM1.03L using the DISS f_oF_2 and h_mF_2 data. The electron density profile extends from 90 to 1000 km. The two initial quiet days look similar, while the strong positive phase of the storm observed both day and night at Ramey is evidently a dominant feature. Of particular note are the strong shears in altitude as the dayside F region rapidly transitions to a nighttime F layer. Such strong shears are also postulated to exist from the in-depth analysis of GPS TEC data during this CIC storm [*Makela et al.*, this issue]. It is well known that in reducing GPS slant TEC to vertical TEC, a knowledge of the F region altitude is crucial [*Lanyi and Roth*, 1988]. The dynamics of the F layer shown in Plate 2 when the layer changes from 270 to almost 400 km in less than 2 hours is a severe problem for such slant-to-vertical inversion procedures.

In using the AIM1.03L simulation only the slant GPS TEC were evaluated. These were, however, evaluated assuming that the instantaneous Ramey AFB DISS assimilated profile applied over the entire field of view of the St. Croix GPS receiver. Figure 6 shows a set of IRI modeled slant TECs (top panel), AIM1.03L modeled slant TECs (middle panel), and GPS pseudorandom number (PRN) 22 slant TEC values (bottom panel). In calculating both AIM1.06L and IRI slant TEC the integration ended at an altitude of 1000 km, and no plasmaspheric contribution was added. A summation of IRI incremental TEC values at 2 km steps along the individual slant ray paths was used to derive the IRI slant TEC. The IRI slant TEC show the expected repetition of the monthly climatology from quiet days through storm days. In contrast, the observations reveal a considerable day-to-day variability as well as structure in each satellite pass. These variations are also present in the AIM1.03L driven by the Ramey Solar Observatory DISS data. PRN 22 is one of five GPS satellites that were observed during a time period when the storm ionosphere showed dramatically different structure than on the quiet days, i.e., Figure 6 quiet-to-storm day TEC path morphological differences. The deep minimum found on the storm days 326 and 327 is reproduced, while in the recovery phase, on day 328, both the minimum and maximum are reproduced. On the first 2 days, days 324 and 325, which correspond to

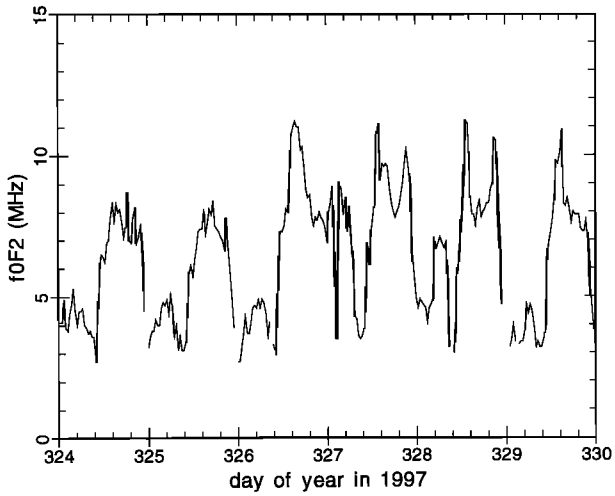

Figure 5. DISS f_oF_2 data from days 324 through 329, 1997, from the Ramey AFB digisonde.

quiet prestorm conditions, all three data sets are somewhat similar. Even on these 2 quiet days the AIM1.03L fits the observations better than the IRI.

A total of 26 separate GPS satellite data sets exist for these days. Figure 7 shows the superposition of these satellite data sets and model slant TEC for the study period. The IRI repetition is obvious. During the quiet days the IRI slant TEC exceeds the GPS values, while at night they are lower. The AIM1.03L slant TEC on the quiet days is lower than the observed GPS TEC during both day and night. On the storm days, in particular, AIM1.03L mimics the observed GPS departures from the quiet days. On days 326, 327, and 328 the enhanced TEC in the afternoon sector is well reproduced. Although on day 326 at 1500 UT the GPS observations reach 100 TEC units which are not reproduced in magnitude, the AIM1.03L model increased from the quiet day value by a factor of 2.1. This compares favorably with the observed GPS TEC increase ratio of 2.0 at this UT.

The issue of absolute GPS TEC is addressed in detail by *Makela et al.* [this issue]. Only a brief description of the specific technique is now given. GPS TEC requires detailed calibration to minimize both receiver and satellite biases as well as to compensate for propagation effects such as multipath. To determine the biases, *Makela et al.* [this issue] used the pseudorange technique described by *Lanyi and Roth* [1988]. Initially, the St. Croix receiver was used as a reference null bias, against which a second receiver bias was determined. The GPS satellite bi-

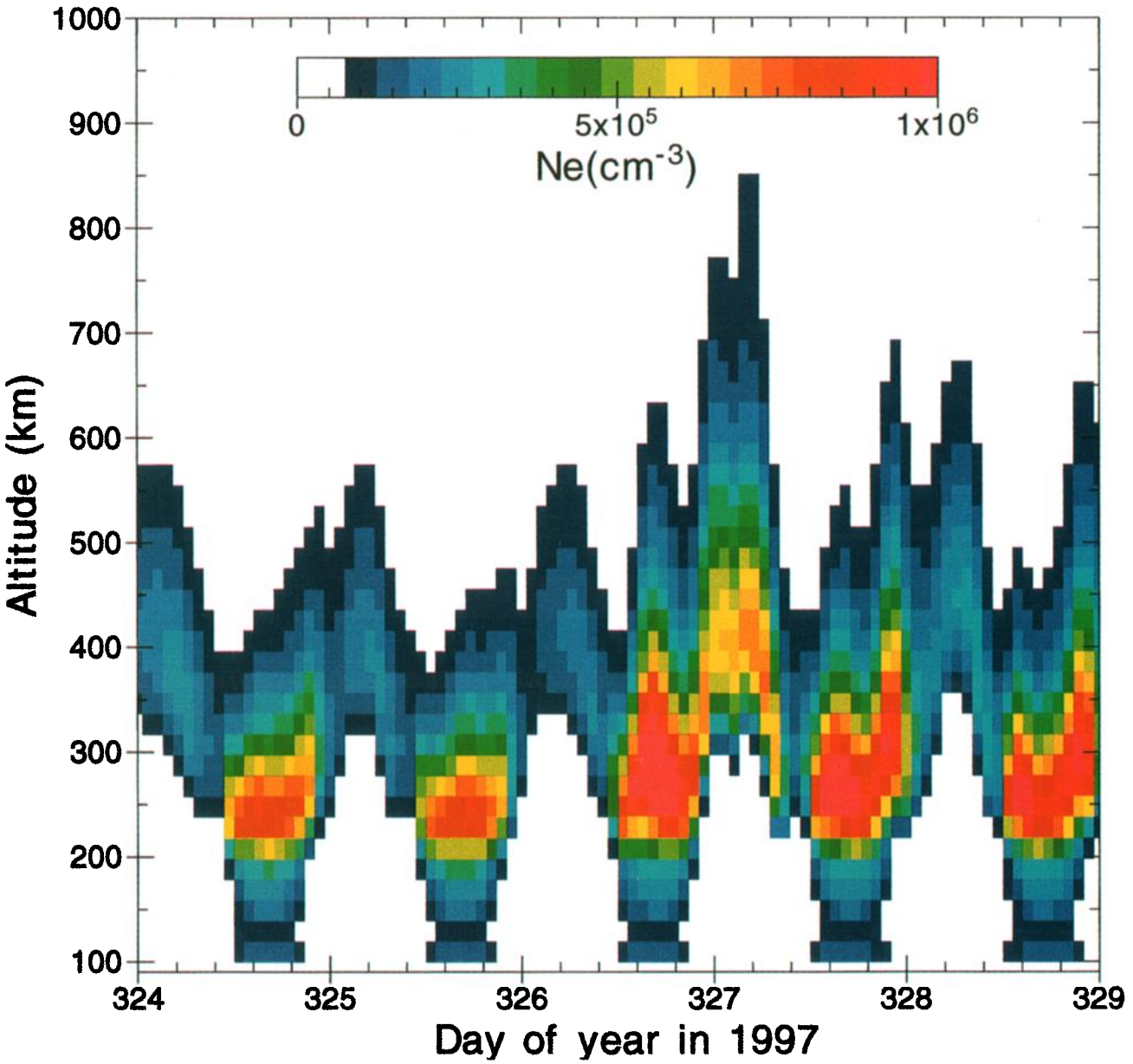

Plate 2. AIM1.03L electron densities for Ramey AFB as a function of altitude from 90 to 1000 km from days 324 through 329. The electron density is plotted linearly both in contour and color formats.

ases from the Jet Propulsion Laboratory (JPL) GPS groups were adopted. Then the final absolute bias of St. Croix and the other station was obtained by cross-calibrating with the JPL global ionospheric maps on quiet days prior to the CIC storm interval. In order to mitigate the multipath problem only slant paths whose elevation angle was greater than 25° were used.

To demonstrate the difference more directly, Figure 8 shows the IRI-GPS slant TEC (top panel), AIM1.03L-GPS slant TEC (middle panel), and then, for reference, a repeat of the GPS slant TEC (bottom panel). In Figure 8 the range of the difference TEC is −30–20 TEC units (TECU), compared to the 0–100 TECU used for the GPS slant TEC. If either model fitted GPS exactly, the difference would be zero, and

a straight line would appear. Neither satisfies this criterion. However, it is clear that the IRI shows systematic departures from the straight line while AIM1.03L tends to have scatter about a relatively straight mean. In the IRI difference the average difference has IRI 4.4 TECU low while the average difference for AIM1.03L is 8.4 TECU. During the storm onset on day 326, around 1500 UT, when GPS slant TEC reaches almost 100 TECU, neither model gets to within 30 TECU. However, this is an example of where the AIM1.03L sees the weather but, because the timing or spatial structure is fine enough, the differences on specific slant paths are still large. The pitfall is that the climatology provides no weather and therefore gives an "average" agreement while a weather model produces structures which, if not

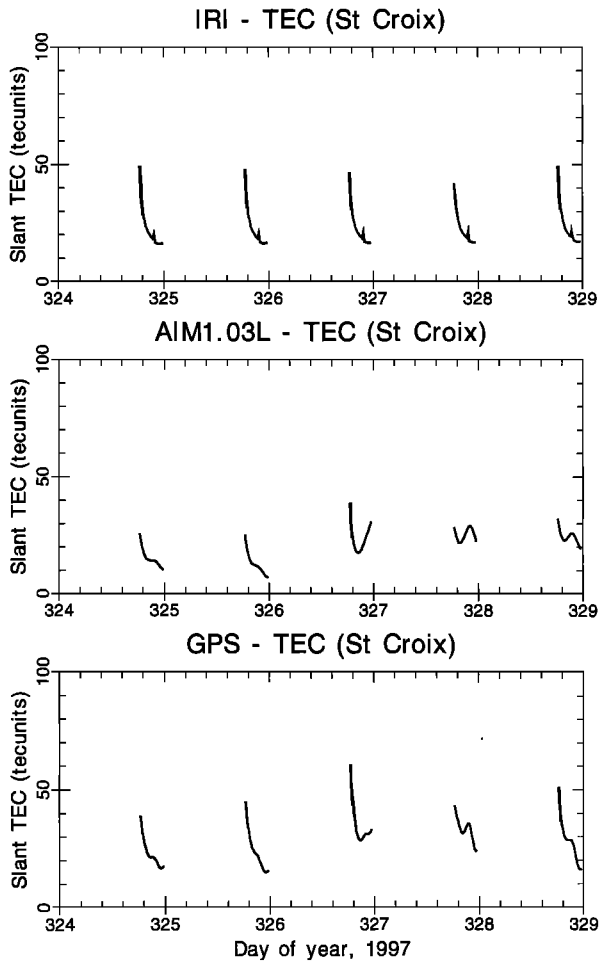

Figure 6. (top) IRI slant TEC, (middle) local AIM1.03L slant TEC, and (bottom) slant TEC from GPS PRN 22 to St. Croix from days 324 through 328, 1997.

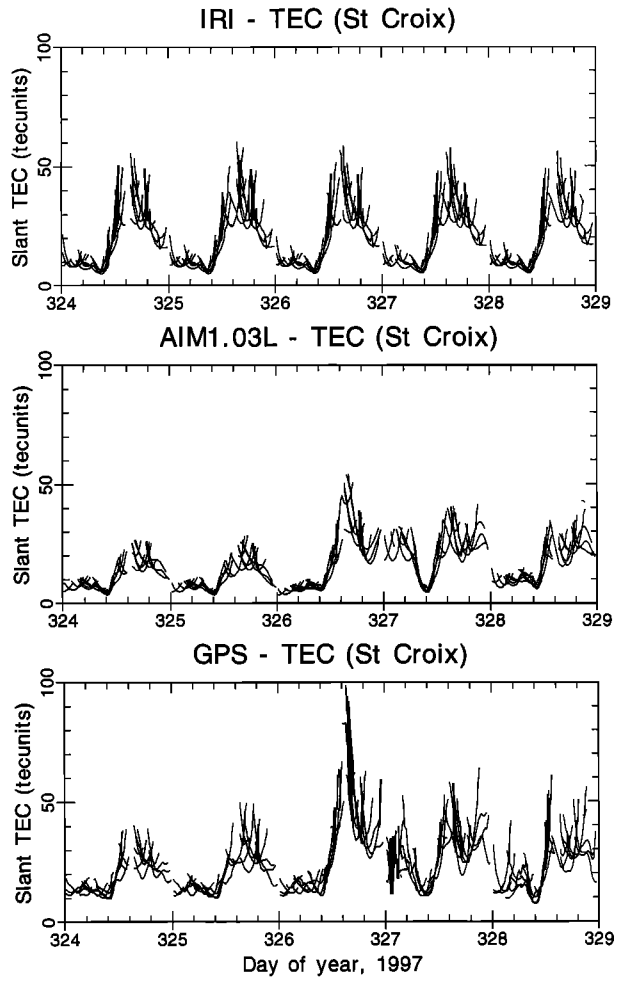

Figure 7. (top) IRI slant TEC, (middle) local AIM1.03L slant TEC, and (bottom) slant TEC from all GPS satellites to St. Croix from day 324 through day 328, 1997.

exactly colocated, will potentially produce "even" larger errors.

6. Conclusion

The study has successfully demonstrated the concept of the first step in ionospheric assimilation, namely, that the use of appropriate observations ingested into a physical model will generate a superior initial estimate of the ionosphere compared to a purely climatological model. This is demonstrated in Figure 7 by comparing the top (IRI) and middle (AIM1.03L) panels with the bottom panel (observations). The weather trends are captured by AIM1.03L. A Kalman filter technique of pure assimilation would be the next step in the ionospheric

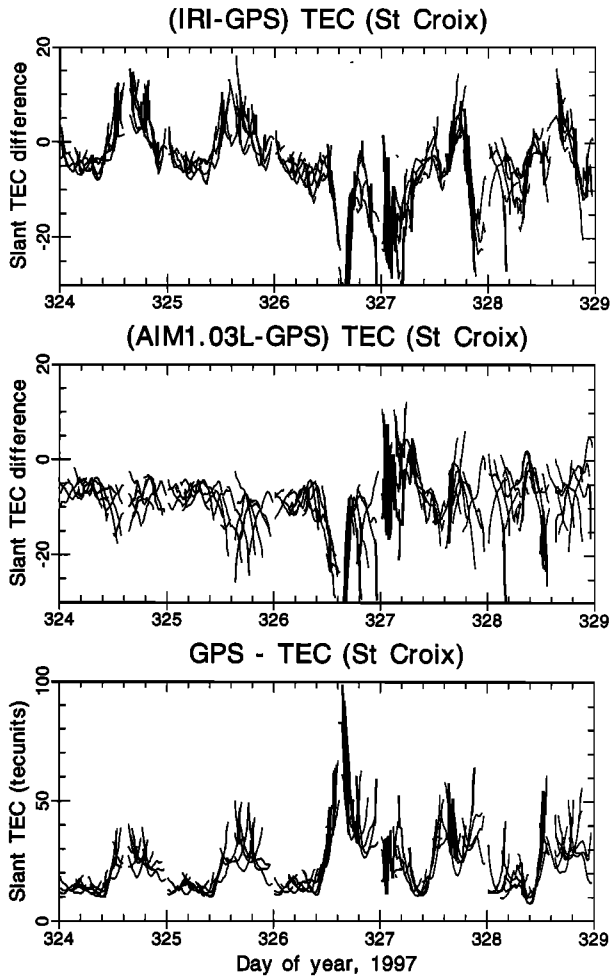

Figure 8. (top) Slant TEC difference plots for IRI and (middle) AIM1.03L relative to GPS, with (bottom) GPS slant TEC. The data are for the period days 324 through 328, 1997.

assimilation. This could be viewed as a "scaling" of the estimate of the ionosphere as represented by the middle panel of Figure 7 with ionospheric observations, such as the slant TEC values of the bottom panel in Figure 7, to produce the final ionospheric specification.

Also shown in this study were the initial results of developing ionosonde ingest algorithms; AIM1.03L and AIM1.03R. These algorithms are not conventional servo class algorithms. They use both f_oF_2 and h_mF_2 information in an iterative sense to evaluate either a local or region-induced plasma drift. In turn, these drifts drive a physical model of the midlatitude ionosphere. Results presented in Figure 2 and Plate 1 demonstrate that this technique is able to track ionospheric weather variations. As a comparison, it was shown that the AIM1.03L model achieves a factor of 2 better accuracy than IRI in terms of the daily f_oF_2 deviation. AIM1.03L f_oF_2 deviations as low as 3% are attainable for summer conditions and rarely exceed 10%. Future improvements to this specific model in the form of nighttime maintenance will act to reduce the 10% error that occurs for winter conditions.

Work is under way to extend the midlatitude AIM ingestion scheme. The immediate upgrade is to include the bottomside ionogram information.

Acknowledgments. This work was supported by contract N00014-98-C-0085 from the Office of Naval Research to Space Environment Corporation. Research at Cornell University was supported under ONR contract N00014-92-J-1822 and, in part, with a National Science Foundation Graduate Research Fellowship.

References

Bilitza, D., International Reference Ionosphere 1990, *Rep. 90-22*, http://nssdc.nasa.gov, Natl. Space Sci. Data Cent., Greenbelt, Md., 1990.

Bilitza, D., N. M. Sheik, and R. Eyfrig, A global model for the height of the F_2-peak using $M3000$ values from the CCIR numerical map, *Telecommun. J., 4b*, 549, 1979.

Buonsanto, M. J., Observed and calculated F_2 peak heights and derived meridional winds at mid-latitudes over a full solar cycle, *J. Atmos. Terr. Phys., 52*, 223–240, 1990.

Buonsanto, M. J., M. J. Starks, J. E. Titheridge, P. G. Richards, and K. L. Miller, Comparison of techniques for derivation of neutral meridional winds from ionospheric data, *J. Geophys. Res., 102*, 14,477–14,484, 1997.

Daley, R., *Atmospheric Data Analysis*, Cambridge Univ. Press, New York, 1990.

Dudeney, J. R., A simple empirical method for estimating the height and semi-thickness of the F-2-layer at the Argentine Islands, Graham Land, *Br. Antarct. Surv. Sci. Rep., 88*, 3–45, 1974.

Hedin, A. E., et al., Revised global model of thermosphere winds using satellite and ground-based observations, *J. Geophys. Res., 96*, 7657–7688, 1991.

Lanyi, G. E., and T. Roth, A comparison of mapped and measured total ionospheric electron content using global positioning system and beacon satellite observations, *Radio Sci., 23*, 483–492, 1988.

Makela, J. J., M. C. Kelley, J. J. Sojka, X. Pi, and A. J. Mannucci, GPS normalization of and preliminary modeling results of total electron content during a midlatitude space weather event, *Radio Sci.*, this issue.

Miller, K. L., D. G. Torr, and P. G. Richards, Meridional

winds in the thermosphere derived from measurement of F_2 layer height, *J. Geophys. Res.*, *91*, 4531–4535, 1986.

Richards, P. G., An improved algorithm for determining netural winds from the height of the F_2 peak electron density, *J. Geophys. Res.*, *96*, 17,839–17,846, 1991.

Rishbeth, H., The effects of winds on the ionospheric F_2-peak, *J. Atmos. Terr. Phys.*, *29*, 225–238, 1967.

Rishbeth, H., S. Ganguly, and J. C. G. Walker, Field-aligned and field-perpendicular velocities in the ionospheric F_2 layer, *J. Atmos. Terr. Phys.*, *40*, 767–784, 1978.

Schunk, R. W., A mathematical model of the middle and high latitude ionosphere, *Pure Appl. Geophys.*, *127*, 255–303, 1988.

Schunk, R. W., J. J. Sojka, and J. V. Eccles, Expanded capabilities for the ionospheric forecast model, *Rep. AFRL-VS-HA-TR-98-0001*, Air Force Lab., Hanscom AFB, Mass., 1997.

Sojka, J. J., Global scale, physical models of the *F*-region ionosphere, *Rev. Geophys.*, *27*, 371–403, 1989.

Titheridge, J. E., The calculation of neutral winds from ionospheric data, *J. Atmos. Terr. Phys.*, *57*, 1015–1036, 1995.

T. W. Bullett, Battlespace Environment Division, Air Force Research Laboratory, Hanscom Air Force Base, MA 01731-3010.

J. J. Makela, Department of Electrical and Computer Engineering, Cornell University, 318 Rhodes Hall, Ithaca, NY 14853-5401.

R. W. Schunk, J. J. Sojka, and D. C. Thompson, Space Environment Corporation, 399 North Main, Suite 325, Logan, UT 84321. (jan@spacenv.com)

(Received December 1, 1999; revised August 8, 2000; accepted August 8, 2000.)